

Text  
page

(1)

## TEMPORAL CHANGES IN ENDMEMBER ABUNDANCES, LIQUID WATER AND WATER VAPOR OVER VEGETATION AT JASPER RIDGE

Dar A. Roberts<sup>1</sup>, Robert O. Green<sup>2</sup>, Donald E. Sabol<sup>1</sup>, John B. Adams<sup>1</sup>

1. Department of Geological Sciences, AJ-20  
University of Washington, Seattle, WA 98195

2. Jet Propulsion Laboratory, California Institute of Technology, Pasadena, CA 91109

### 1. INTRODUCTION

Imaging spectrometry offers a new way of deriving ecological information about vegetation communities from remote sensing. Applications include derivation of canopy chemistry (e.g., Wessman et al., 1989), measurement of column atmospheric water vapor and liquid water (Green et al., 1991), improved detectability of materials (Sabol et al., 1992), more accurate estimation of green vegetation cover and discrimination of spectrally distinct green leaf, non-photosynthetic vegetation (NPV: litter, wood, bark etc.) and shade spectra associated with different vegetation communities (Roberts et al., 1993).

Much of our emphasis has been on interpreting Airborne Visible and Infrared imaging Spectrometry (AVIRIS) data as spectral mixtures. Two approaches have been used, simple models, where the data are treated as a mixture of 3 to 4 laboratory/field measured spectra, known as reference endmembers (EMs), applied uniformly to the whole image, to more complex models where both the number of EMs and the types of EMs vary on a per-pixel basis (Roberts et al., 1992). Where simple models are applied, materials, such as NPV, which are spectrally similar to soils, can be discriminated on the basis of residual spectra (Roberts et al., 1993). One key aspect is that the data are calibrated to reflectance and modeled as mixtures of reference EMs, permitting temporal comparison of EM fractions, independent of scene location or data type. In previous studies the calibration was performed using a modified-empirical line calibration (Roberts et al., 1993), assuming a uniform atmosphere across the scene.

In this study, a Modtran-based calibration approach was used to map liquid water and atmospheric water vapor and retrieve surface reflectance from three AVIRIS scenes acquired in 1992 over the Jasper Ridge Biological Preserve (see Green et al., 1993). The data were acquired on June, 2nd, September 4th and October 6th. Reflectance images were analyzed as spectral mixtures of reference EMs using a simple 4 EM model. Atmospheric water vapor derived from Modtran was compared to elevation, and community type. Liquid water was compared to the abundance of NPV, Shade and Green Vegetation (GV) for select sites to determine whether a relationship existed, and under what conditions the relationship broke down. Temporal trends in endmember fractions, liquid water and atmospheric water vapor were investigated also. The combination of spectral mixture analysis and the Modtran based atmospheric/liquid water models was used to develop a unique vegetation community description.

### 2. RESULTS

Atmospheric water vapor, liquid water and the abundance of soil, NPV, GV and photometric shade, were determined for 14 sites of known elevation from the 3 dates (Fig. 1). A comparison of atmospheric water vapor to elevation demonstrated a good linear relationship for all 3 dates, with September having the highest water vapor

concentrations, June intermediate and October the lowest (Fig. 2). Atmospheric water vapor was negatively correlated to increased elevation. The steepest gradient occurred at intermediate water vapor concentrations in June, producing the highest contrast between elevations. The relationship between elevation and atmospheric water vapor showed a marked departure from predicted water vapor over heavily vegetated areas in June and September. In all of the study regions, except the Stanford Golf Course (C in Fig. 1), the atmospheric water vapor was higher over the vegetated regions. These departures may represent evaporated water vapor, trapped water vapor in canyons or an incomplete separation of liquid water from atmospheric water vapor. The latter, however, is unlikely, because liquid water and atmospheric water vapor, although positively correlated, were not directly correlated in all areas. Liquid water was mapped as showing very sharp gradients between vegetated and non-vegetated areas. Atmospheric water vapor, on the other hand, had gradational boundaries. Heavily vegetated sites did not show above normal water vapor concentrations on the driest date, in October, potentially attributable to low transpiration rates at that time.

### Figure 1

Figure 1. Index map showing the location of 10 of the study sites. These include a Horse Ranch (A), Webb Ranch (B), Stanford Golf Course (C), Evergreen Broadleaf Forest (D), Serpentine Grassland (E), Chaparral (F), Annual Grassland (G), Forested Wetland (H) and 3 high elevation grasslands (I, J and K). Four forested areas in the Santa Cruz Mountains, one at Alambique Creek (317 m), and three along an elevational transect in Martin Creek, at 183, 212 and 390 m, respectively, were off the map.

The EM fractions changed among the three dates, primarily due to a decrease in the solar elevation and senescence, producing an increase in the shade and NPV fractions and a decrease in the GV fraction (Fig. 3, Site locations, Fig. 1). For a more detailed discussion of the relationship between endmember abundances, vegetation communities, and temporal trends see Sabo et al. (1993).

Fractions of NPV, GV and shade were compared to liquid water absorptions for the three dates (Fig. 4a-c). The best relationships occurred in June, where shade and GV were positively correlated to liquid water and NPV was negatively correlated. The best fit was for NPV and liquid water. The only major departure was in the Serpentine site (E) on

Fig. 1), where the soil fraction was high. GV showed departures at two sites, the Stanford Golf Course, where the GV fraction was high, but the liquid water concentration low, and in the Santa Cruz Mountains (Martin and Alambique Creeks), where the highest liquid water absorptions occurred but GV was low due to a high shade fraction ( $>0.60$ ). In these areas, shade showed a high correlation with liquid water. The difference between GV and liquid water absorption is due, most likely, to the low leaf area of the golf course grasses. The relationship between the EM fractions was similar for the other two dates, although the fit was poorer. Liquid water absorption showed a systematic change, between the three dates; values for September were higher than June by 20, whereas the October values were lower for the lowest sites (by approximately 10) and slightly higher for the sites with the highest absorption. Whether these differences are real (due to rainfall in September), or due to modeling errors (e.g., slight wavelength miscalibrations) requires further investigation.

Figure 2. Comparison between atmospheric water vapor and elevation for the 14 study sites over the three dates. Water vapor was negatively correlated with elevation (June:  $Y = -1.236 \cdot X + 1820$ ,  $R^2 = 0.966$ ; Sept:  $Y = -0.759 \cdot X + 2225$ ,  $R^2 = 0.875$ ; Oct.:  $Y = -0.576 \cdot X + 1117$ ,  $R^2 = 0.896$ ).

Figure 3. Changes in endmember fractions at 7 sites on three dates. The first, second and third columns are for June, next three for September and last three for October. Negative and super-positive ( $>1.0$ ) fractions are due to limitations in the simple model (see Sabolet et al., 1993).

### 3. SUMMARY

AVIRIS provides information about vegetation that cannot be obtained using other sensors. In this paper we mapped temporal and spatial patterns in liquid water,

atmospheric water vapor, shade, GV, NPV and soil, relating these parameters to vegetation types. Examples included atmospheric water vapor which was modeled as higher, for a given elevation, over vegetated sites than non-vegetated sites for June and September, but not for October, on a dryer day. Liquid water was correlated with GV on all three dates except for highly shaded areas, where shade showed a better relationship, and areas with low leaf area but a high GV fraction, such as the Stanford Golf Course. Under these instances, liquid water estimates and mixture models provide complementary, but different information about vegetation. Through this analysis, we offer a new way to characterize vegetation communities through their physical attributes (LW fractions and liquid water) and associated atmospheric properties (water vapor).

Figure 4. Scatterplot between scaled liquid water absorption and NPV, GV and Shade fractions. For all three dates, NPV was negatively correlated and shade and GV were positively correlated

4. REFERENCES

Green, R.O., Conel, J.E., Margolis, I. S., Bruegge, C. J., and Hoover, G.L., An Inversion Algorithm for Retrieval of Atmospheric and Leaf Water Absorption from AVIRIS Radiance With Compensation for Atmospheric Scattering. *Summaries of the 3rd Annual JPL Airborne Geoscience Workshop, vol. 1, AVIRIS Workshop* (Green ed.), 11<sup>th</sup>. Publication 92-14, Jet Propulsion Laboratory, Pasadena, CA, June 1, 1992, pp. 51-61.

Green, R.O., Conel, J.E. and Roberts, D.A., 1993, Estimation of Aerosol Optical Depth and Calculation of Apparent Surface Reflectance from Radiance Measured by the Airborne Visible-Infrared Imaging Spectrometer (AVIRIS) Using MODTRAN2", *SPIE Conf. 1937, Imaging Spectrometry of the Terrestrial Environment*, in press, 12 p.

Roberts, D. A., Smith, M.O., Sabol, D.E., Adams, J.B., and Ustin, S., Mapping the Spectral Variability in Photosynthetic and Non-photosynthetic Vegetation, Soils and Shade Using AVIRIS, *Summaries of the 3rd Annual JPL Airborne Geoscience Workshop, vol. 1, AVIRIS Workshop* (Green ed.), 11<sup>th</sup>. Publication 92-14, Jet Propulsion Laboratory, Pasadena, CA, June 1, 1992, pp. 38-40.

Roberts, D. A., Smith, M.O., and Adams, J.B., 1993, Green Vegetation, Nonphotosynthetic Vegetation, and Soils in AVIRIS Data. *Remote Sens. Environ.*, 44:255-269.

Sabol, D.E., Adams, J.B., and Smith, M.O., 1992, Quantitative Subpixel Spectral Detection of Targets in Multispectral Images. *J. Geophys. Res.*, 97(12): 2659-2672.

Sabol, D.E., Roberts, D. A., Adams, J.B., and Smith, M.O., 1993, Mapping and Monitoring Changes in Vegetation Communities of Jasper Ridge, CA. Using Spectral Fractions, this volume.

Wessman, C. A., Aber, J.D., and Peterson, D.J., 1989. An Evaluation of Imaging Spectrometry for Estimating Forest Canopy Chemistry. *Int. J. Remote Sens.*, 10(8): 1293-1316.

Page with  
art only

5

concentrations, June intermediate and October the lowest (Fig. 2). Atmospheric water vapor was negatively correlated to increased elevation. The steepest gradient occurred at intermediate water vapor concentrations in June, producing the highest contrast between elevations. The relationship between elevation and atmospheric water vapor showed a marked departure from predicted water vapor over heavily vegetated areas in June and September. In all of these regions, except the Stanford Golf Course (C in Fig. 1), the atmospheric water vapor was higher over the vegetated regions. These departures may represent evapotranspired water vapor, trapped water vapor in canyons or an incomplete separation of liquid water from atmospheric water vapor. The latter, however, is unlikely, because liquid water and atmospheric water vapor, although positively correlated, were not directly correlated in all areas. Liquid water was mapped as showing very sharp gradients between vegetated and non-vegetated areas. Atmospheric water vapor, on the other hand, had gradual boundaries. In heavily vegetated sites did not show above normal water vapor concentrations on the driest date, in October, potentially attributable to low transpiration rates at that time.

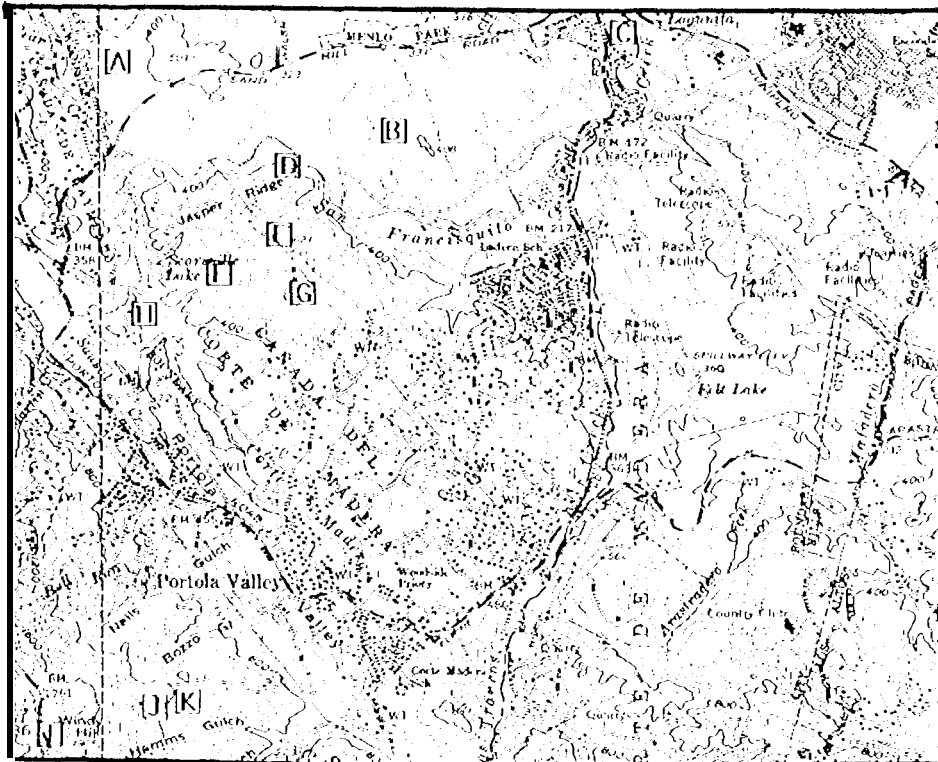


Figure 1. Index map showing the location of 10 of the study sites. These include a Horse Ranch (A), Webb Ranch (B), Stanford Golf Course (C), Evergreen Broadleaf Forest (D), Serpentine Grassland (E), Chaparral (F), Annual Grassland (G), Forested Wetland (H) and 3 high elevation grasslands (I, J and K). Four fenced areas in the Santa Cruz Mountains, one at Alambique Creek (317 m), and three along an elevational transect in Martin Creek, at 183, 262 and 390 m, respectively, were off the map.

The EM fractions changed among the three dates, primarily due to a decrease in the solar elevation and senescence, producing an increase in the shade and NPV fractions and a decrease in the GV fraction (Fig. 3, Site locations, Fig. 1). For a more detailed discussion of the relationship between member abundances, vegetation communities, and temporal trends see Sabol et al. (1993).

Fractions of NPV, GV and shade were compared to liquid water absorptions for the three dates (Fig. 4a-c). The best relationships occurred June, where shade and GV were positively correlated to liquid water and NPV was negatively correlated. The best fit was for NPV and liquid water. The only major departure was in the Serpentine site (E)

Page with and only

(6)

on Fig. 1), where the soil fraction was high. GV showed departures at two sites, the Stanford Golf Course, where the GV fraction was high, but the liquid water concentration 10W, and in the Santa Cruz Mountains (Martin and Alambique [kinks]), where the highest liquid water absorptions occurred but GV was low due to a high shade fraction (> 0.60). In these areas, shade showed a high correlation with liquid water. The difference between GV and liquid water absorption is due, most likely, to the low leaf area of the golf course grasses. The relationship between the EM fractions was similar for the other two dates, although the fit was poorer. Liquid water absorption showed a systematic change between the three dates; values for September were higher than June by 20, whereas the October values were lower for the lowest silts (by approximately 10) and slightly higher for the sites with the highest absorptions. Whether these differences are real (due to rainfall in September), or due to modeling errors (e.g., slight wavelength miscalibrations) requires further investigation.

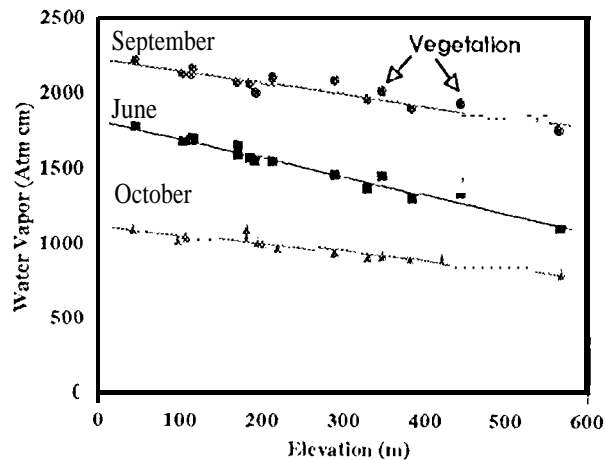


Figure 2. Comparison between atmospheric water vapor and elevation for the 14 study sites over the three dates. Water vapor was negatively correlated with elevation (June:  $Y = -1.236 \cdot X + 1820$ ,  $R^2 = 0.966$ ; Sept:  $Y = -0.759 \cdot X + 2225$ ,  $R^2 = 0.875$ ; Oct.:  $Y = -0.576 \cdot X + 1117$ ,  $R^2 = 0.896$ ).

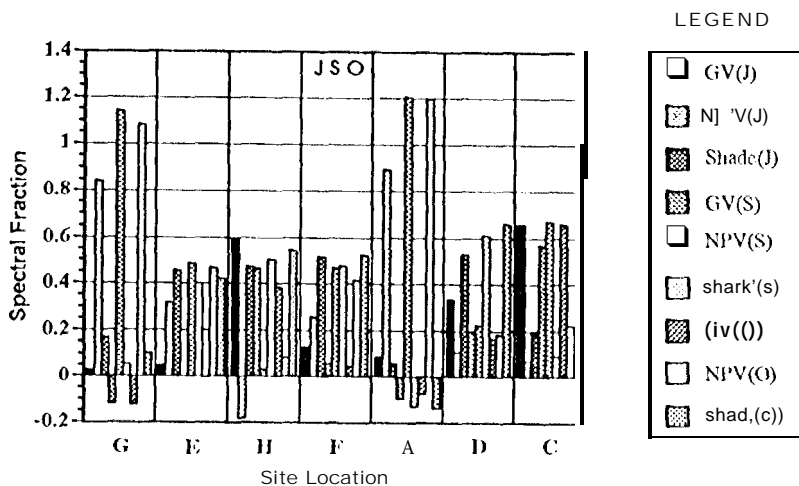


Figure 3. Changes in endmember fractions at 7 sites on three dates. The first, second and third columns are for June, next three for September and last three for October. Negative and super-positive (> 1.0) fractions are due to limitations in the simple model (see Sabol et al., 1993).

### 3. SUMMARY

AVIRIS provides information about vegetation that cannot be obtained using other sensors. In this paper we mapped temporal and spatial patterns in liquid water,

atmospheric water vapor, shade, GV, NPV and soil, relating these parameters to vegetation types. Examples included atmospheric water vapor which was modeled as higher, for a given elevation, over vegetated sites than on-vegetated sites for June and September, but not for October, on a dryer day. Liquid water was correlated with GV on all three dates except for highly shaded areas, where shade showed a better relationship, and areas with low leaf area but a high GV fraction, such as the Stanford Golf Course. Under these instances, liquid water estimates and mixture models provide complimentary, but different information about vegetation. Through this analysis, we offer a new way to characterize vegetation communities through their physical attributes (L:M fractions and liquid water) and associated atmospheric properties (water vapor).

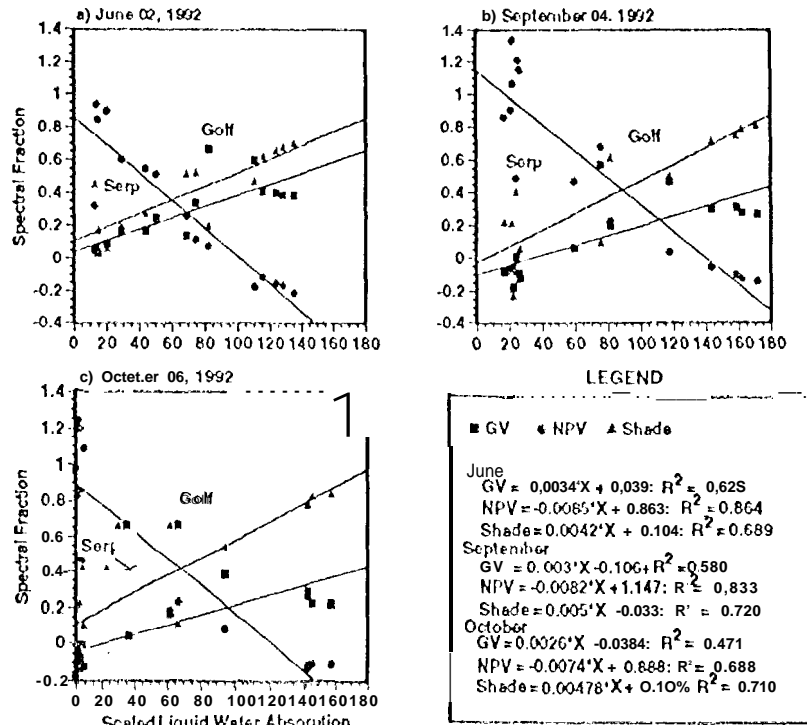


Figure 4. Scatter plot between scaled liquid water absorption and NPV, GV and Shade fraction for all three dates. NPV was negatively correlated and shade and GV were positively correlated

#### 4. REFERENCES

- Keen, R.O., Conel, J.E., Margolis, J.S., Bruegge, C.J., and Hoover, C.A., An Inversion Algorithm for Retrieval of Atmospheric and Leaf Water Absorption From AVIRIS Radiance With Compensation for Atmospheric Scattering, *Proc. 3rd AVIRIS Workshop* (Green ed.), Pasadena, CA, May 20-21, 1991, pp. 51-61.
- Green, R. C., Conel, J.E. and Roberts, D. A., 1993, Estimation of Aerosol Optical Depth and Calculation of Apparent Surface Reflectance from Radiance Measured by the Airborne Visible-Infrared Imaging Spectrometer (AVIRIS) Using MODTRAN2", *SPIE Conf. 1937, Imaging Spectrometry of the Terrestrial Environment*, in press, 2 p.
- Roberts, D.A., Smith, M.O., Sabol, D.E., Adams, J. B., and Ustin, S., Mapping the Spectral Variability in Photosynthetic and Non-photosynthetic Vegetation, Soils and Shade Using AVIRIS, *Proc. 3rd Airborne Geoscience Workshop* (Green ed.), Pasadena, CA, June 1-5, 1992, pp. 38-40.
- Roberts, D.A., Smith, M.O., and Adams, J.B., 1993, Green Vegetation, Nonphotosynthetic Vegetation, and Soils in AVIRIS Data. *Remote Sens. Environ.*, 44:255-269.
- Sabol, D.E., Adams, J.B., and Smith, M.O., 1992, Quantitative Subpixel Spectral Detection of Targets in Multispectral Images. *J. Geophys. Res.*, 97(12): 2689-2672.
- Sabol, D.E., Roberts, D. A., Adams, J.B., and Smith, M.O., 1993, Mapping and Monitoring Changes in Vegetation Communities of Jasper Ridge, CA, Using Spectral Fractions, this volume.
- Wessman, C.A., Aber, J.D., and Peterson, D.J., 1989, A Evaluation of Imaging Spectrometry for Estimating Forest Canopy Chemistry. *Int. J. Remote Sens.*, 10(8): 1293-1316.